A. Muzhikyan, A. M. Farid, and K. Youcef-Toumi, "A Power Grid Enterprise Control Method for Energy Storage System Integration," in IEEE Innovative Smart Grid Technologies Conference Europe, (Istanbul, Turkey), pp. 1–6, 2014.

A Power Grid Enterprise Control Method for Energy Storage System Integration

Aramazd Muzhikyan[1], Amro M. Farid[2] and Kamal Youcef-Toumi[3]

***Abstract*—Traditionally, power system balancing operations consist of three consecutive control techniques, namely security-constrained unit commitment (SCUC), security constrained economic dispatch (SCED), and automatic generation control (AGC). Each of these have their corresponding type of operating reserves. Similarly, energy storage systems (ESS) may be integrated as energy, load following, or regulation resources. A review of the existing literature shows that most ESS integration studies are focused on a single control function. In contrast, recent work on renewable energy integration has employed the concept of enterprise control where the multiple layers of balancing operations have been integrated into a single model to capture and potentially control the interactions between timescales. This paper now uses such an enterprise control model to demonstrate the multiple timescale effects as a consequence of ESS integration into a single control action. It also proposes a novel scheduling technique which beneficially exploits this coupling in two timescales. As a result, the ESS scheduling technique shows peak-loading shaving and operating costs reductions in the SCUC and load following reserve requirements in the SCED.**

***Keywords*—Energy storage systems, enterprise control**

I. Introduction

Traditionally, power system balancing operations consist of three consecutive control techniques, namely, security-constrained unit commitment (SCUC), security-constrained economic dispatch (SCED) and automatic generation control (AGC), where each consecutive control operates at a faster timescale [1]. The power system operator keeps the generation and consumption balance in the system by scheduling sufficient amounts of load following, ramping and regulation reserves. Each of these is applied to an individual control technique. However, these control activities are often coupled and therefore analyses restricted to a single control action do not give a complete picture of the evolution and development of power system imbalances [2]. Recently, power grid *enterprise control* modeling has been developed to holistically incorporate the multiple layers of balancing operations; thus capturing the control interactions at different timescales. The benefits of holistic power system modeling have been demonstrated in renewable energy integration, the determination of imbalances and the assessment of reserve requirements [3], [4].

Similar to power system reserves, energy storage systems (ESS) can have various applications in power system operation and control, depending on their type and physical characteristics [5], [6]. Within the scope of this paper, three ESS integration applications are considered: 1.) as an energy resource in the unit commitment model, 2.) as a load following resource, 3.) as a regulation resource. Integration into the unit commitment model accomplishes several goals simultaneously. Besides peak-load shaving and system operating cost reduction, the inclusion of additional constraints can also lead to emission and congestion reduction [7], [8]. Integration of ESS as a load following resources reduces the actual load following requirements hence the system cost. Two types of operation modes can be chosen: fixed pattern and load following [9]. When choosing the operating mode, there is a tradeoff between the risk of battery shortage/surplus and the quality of the imbalance mitigation. The ESS ramping capabilities should be considered when implemented as a regulation service. A simple control mechanism of the ESS frequency regulation stores/provides energy when the area control error (ACE) exceeds its higher/lower bounds [10].

A review of the existing ESS literature shows that most studies are focused on a single time scale [5], [6]. It is implicitly assumed that the impact of ESS integration into a given control technique is restricted to its associated timescale; thus neglect potential interactions between timescales. As a result, the possible benefits of the ESS integration that lie outside the scope are missed. Similarly, the possible negative impacts on the adjacent timescales are also ignored.

The purpose of this paper is two-fold: 1.) to demonstrate the effect of ESS integration into a single control action on multiple timescales and 2.) to propose a novel scheduling technique which beneficially exploits this coupling in two timescales. More specifically, the ESS scheduling technique introduced in this paper shows peak-load shaving and operation cost reduction as part of the SCUC. Meanwhile, it reduces load following reserve requirements in the SCED. Observing these interactions is made possible by the modeling of the power system as an enterprise control. As presented in [11], [12], the load following and ramping reserve requirements depend on two factors, the day-ahead forecast error and the limited resolution of the SCUC. Mitigation of the latter effect allows the reduction of the load following reserve requirements. Although the sizing and pricing of the ESS are key components of integration studies [13], [14], it is left outside the scope of this paper.

This paper is organized as follows. Section II presents the background knowledge on the power system control mechanisms and timescales. Also, the information is provided on the scheduling of each type of reserves and their dependance on system properties. Section III presents the methodology of the storage integration into the SCUC problem. Section IV

[1]Aramazd Muzhikyan is with the Department of Engineering Systems and Management, Masdar Institute of Science and Technology, PO Box 54224, Abu Dhabi, UAE amuzhikyan@masdar.ac.ae

[2]Amro M. Farid is with Faculty of Engineering Systems and Management, Masdar Institute of Science and Technology, PO Box 54224, Abu Dhabi, UAE afarid@masdar.ac.ae

[3]Kamal Youcef-Toumi is with Faculty of Mechanical Engineering, Massachusetts Institute of Technology, 77 Massachusetts Avenue Cambridge, MA 02139, USA youcef@mit.edu

presents the simulation results for a single scenario of ESS integration. Section V presents the conclusions.

II. Background

Traditionally, power system balancing operations are formed as a hierarchy of controls: primary, secondary and tertiary [1]. The primary control addresses transient stability phenomena in the range of $10-0.1Hz$ [15]. The secondary control, referred to as automatic generation control (AGC), interacts with the dispatched generators in the control area to maintain the power balance and the system frequency, and acts in a timescale of $20s-2min$. Tertiary control is normally implemented as a security-constrained economic dispatch (SCED) and provides power set-points to the generators ($5-15min$). Balancing operations also include day-ahead scheduling which is commonly implemented as a security-constrained unit commitment (SCUC). This section presents each of these controls in detail.

A. Security-Constrained Unit Commitment (SCUC)

The SCUC problem determines the set of generation units that meet the real-time demand with minimum cost. In the original formulation, the SCUC problem is a nonlinear optimization problem [16]. The cost of generation units is approximated as a quadratic function in the following form:

$$C(P) = C^F + C^L P + C^Q P^2 \tag{1}$$

where C^F, C^L and C^Q are fixed, linear and quadratic cost coefficients respectively. The nonlinear formulation is often linearized to avoid convergence issues:

$$\min \quad \sum_{t=1}^{24}\sum_{i=1}^{N_G}\left(w_{it}C_i^F + C_i^L P_{it} + w_{it}^u C_i^U + w_{it}^d C_i^D\right) \tag{2}$$

$$\text{s.t.} \quad \sum_{i=1}^{N_G} P_{it} = \hat{D}_t \tag{3}$$

$$R_i^{min}T_h \le P_{it} - P_{i,t-1} \le R_i^{max}T_h \tag{4}$$

$$w_{it}P_i^{min} \le P_{it} \le w_{it}P_i^{max} \tag{5}$$

$$w_{it} = w_{i,t-1} + w_{it}^u - w_{it}^d \tag{6}$$

$$\sum_{i=1}^{N_G} w_{it}P_i^{max} - \sum_{i=1}^{N_G} P_{it} \ge P_{res} \tag{7}$$

where the following notations are used:

C_i^U, C_i^D	startup and shutdown costs of generator i
P_{it}	power output of generator i at time t
$\hat{D}_t$	total demand forecast at time t
P_i^{max}, P_i^{min}	max/min power limits of generator i
R_i^{max}, R_i^{min}	max/min ramping rate of generator i
T_h	scheduling time step, normally, 1 hour
N_G	number of generators
w_{it}	ON/OFF state of the generator i
w_{it}^u, w_{it}^d	startup/shutdown indicators of generator i
P_{res}	system reserve requirements

Constraint (3) corresponds to the power balance equation. Constraints (4) and (5) are the limits of the generators' ramping rates and power outputs respectively. The last constraint ensures procurement of the load following reserves.

B. Security-Constrained Economic Dispatch (SCED)

Originally, generation dispatch is a non-linear optimization model, called AC optimal power flow (ACOPF) [17]. Recently, most of the U.S. independent system operators (ISO) moved from ACOPF to linear optimization models to avoid problems with convergence and computational complexity [16]. Security-constrained economic dispatch (SCED) is a commonly used linear optimization model and is formulated as follows [18]:

$$\min \quad \sum_{i=1}^{N_G}(C_i^L \Delta P_{it} + 2C_i^Q P_{it}\Delta P_{it}) \tag{8}$$

$$\text{s.t.} \quad \Delta P_{jt} = \sum_{i=1}^{N_G} B_{ji}\Delta P_{it} \tag{9}$$

$$\sum_{j=1}^{N_B}(1-\gamma_{jt})(\Delta P_{jt} - \Delta D_{jt}) = 0 \tag{10}$$

$$\sum_{j=1}^{N_B} a_{ljt}(\Delta P_{jt} - \Delta D_{jt}) \le F_l^{max} - F_{lt} \tag{11}$$

$$P_{it} - P_i^{min} \le \Delta P_{it} \le P_i^{max} - P_{it} \tag{12}$$

$$R_i^{min}T_m \le \Delta P_{it} \le R_i^{max}T_m \tag{13}$$

where the following notations are used:

ΔP_{it}	power increment of generation i
$\Delta P_{jt}, \Delta D_{jt}$	generation and load increment on bus j
B_{ji}	correspondence matrix of generator i to bus j
F_{lt}, F_l^{max}	power flow level and flow limit of line l
γ_{it}	incremental transmission loss factor of bus i
a_{lit}	bus i generation shift distribution factor to line l
N_B	number of buses
T_m	real-time market time step, normally, 5 minutes.

Sensitivity factors establish linear connections between changes of power injections on the buses and state-related parameters of the system [19]. The incremental transmission loss factor (ITLF) for bus i shows how much the total system losses change, when power injection on bus i increases by a unit [20]. The incorporation of ITLF into the model results in a linearization of the power balance constraint (10). The generation shift distribution factor (GSDF) shows how much the active power flow through line l changes, when injection on bus i increases by a unit [20], [21]. The incorporation of GDSF into the model results in a linearization of the line flow limit constraint (11). Constraints (13) and (12) are the physical limits of the generator ramping rates and outputs.

C. Automatic Generation Control (AGC)

The automatic generation control is generally represented by a dynamic model in combination with generator, prime mover and governor dynamic models [22]. AGC automatically responds to the imbalances of the system and moves the generation units in the opposite direction to mitigate imbalances. The generation units that are controlled by AGC are providing

regulation service to the system. The amount of regulation reserves is defined in advance and the appropriate generation units are selected in the ancillary service market.

III. Methodology

As already mentioned above, the observation of phenomena in different timescales requires a holistic approach to the power system modeling. To this end, this paper utilizes a slightly modified version of the power system enterprise control model proposed in [23], [24]. The modifications are made in the unit commitment by adding storage scheduling and by replacing the linear cost function with a quadratic one. In this section, the SCUC model is detailed. Additionally, a novel ESS scheduling technique is presented to maximize the utilization of the ESS and enhance its impact across timescales.

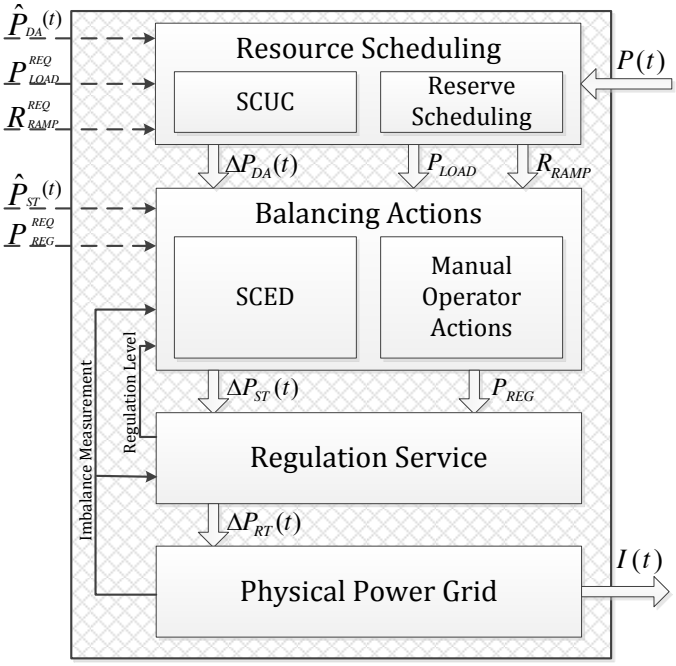

Figure 1: A three layer power grid enterprise control model

A. ESS Integration into SCUC

This study uses the following formulation of SCUC with integrated ESS:

$$\min \quad \sum_{t=1}^{24}\sum_{i=1}^{N_G}(w_{it}C_i^F + C_i^L P_{it} + C_i^Q P_{it}^2 + C_i^U w_{it}^u + C_i^D w_{it}^d) \tag{14}$$

$$\text{s.t.} \quad \sum_{i=1}^{N_G} P_{it} + S_t = \hat{D}_t \tag{15}$$

$$X_t = X_{t-1} - \frac{S_t T_h}{d} \tag{16}$$

$$X_0 = X_{24} \tag{17}$$

$$w_{it}P_i^{min} \le P_{it} \le w_{it}P_i^{max} \tag{18}$$

$$R_i^{min}T_h \le P_{it} - P_{i,t-1} \le R_i^{max}T_h \tag{19}$$

$$S^{min} \le S_t \le S^{max} \tag{20}$$

$$X^{min} \le X_t d \le X^{max} \tag{21}$$

$$w_{it} = w_{i,t-1} + w_{it}^u - w_{it}^d \tag{22}$$

$$\sum_{i=1}^{N_G} w_{it}P_i^{max} - \sum_{i=1}^{N_G} P_{it} \ge P_{res} \tag{23}$$

where the following notations are used in addition to those already defined:

S_t	ESS power output/input at time t
X_t	ESS state of charge (SOC) at time t
S^{min}, S^{max}	ESS power limits
X^{min}, X^{max}	ESS state of charge limits, 0.1-0.9
d	ESS size in MWh

Relative to the SCUC model in Section II, modifications are made to both the objective function and the constraints. The quadratic term is added to the cost function, which makes SCUC a mixed-integer quadratic constraint program (MIQCP). Integration of the quadratic term is necessary to emphasize the economic feasibility of the peak-load shaving. The additional constraints include ESS power and energy limits. Constraint (17) makes sure that the ESS returns to its initial state at the end of the operation day.

B. ESS Scheduling

The SCUC problem returns the hourly values of the generation and storage schedules. Due to the limited time resolution of the SCUC problem, the generation schedule has a stair-like profile in real-time. And yet, this stair-like profile does not capture the overall intra-period rising and falling trends. As a result, and even in the absence of forecast error, load following reserves must be deployed in the SCED so that the generation schedule matches the relatively smooth real-time demand profile [11].

This paper exploits the flexibility of ESS to develop a scheduling technique as a post-process to the SCUC. In addition to the traditional benefits of peak load shaving and operating cost reductions, this technique also simultaneously reduces the load following reserves utilized in the SCED timescale. The main idea behind this technique is that load following reserves can be reduced by feeding the ESS a piecewise linear function that is compatible wight he SCUC result instead of relying on the stair-like (i.e. piecewise constant) profile. As this function is developed, three constraints must be respected. Qualitatively, they are:

Constraint 1: The new schedule and the SCUC result must have the same net energy exchanged within any given SCUC time period T_h.

Constraint 2: The ESS can not exceed its energy storage limit at any moment.

Constraint 3: The ESS can not exceed its power limit at any moment.

1) The Desired Schedule: While the integration of ESS into the SCUC problem reduces the total generation cost, its scheduling flexibility can be also used to reduce the load following requirements of the system. As already mentioned above, the stair-like profile of the generation schedule is one of the factors that affects the load following requirements.

To this end, the desired ESS schedule should ideally make $generation + ESS$ schedule smooth:

$$Z(t) = P(t) + S(t) \tag{24}$$

The smooth profile $Z(t)$ is represented by the following expansion:

$$Z(t) = \sum_{n=-\infty}^{\infty} C_n \hat{f}_n(t) \tag{25}$$

where $\hat{f}_n(t)$ are "piecewise linear harmonic" functions derived from the Fourier series. Consider the the family of n harmonic functions $f_n(t)$

$$f_n(t) = e^{i\frac{2\pi nt}{NT_h}} \tag{26}$$

They may be sampled at the time step of the real-time market T_m to give:

$$f_{n\kappa} = f_n(\kappa T_m) \tag{27}$$

Piecewise linear functions are then defined around these point values.

$$\hat{f}_n(t) = f_{n\kappa} + \frac{t - \kappa T_m}{T_m}\left(f_{n,\kappa+1} - f_{n\kappa}\right), \kappa T_m \le t \le (\kappa+1)T_m \tag{28}$$

where $k = 0, 1, \ldots, N_m$. N_m is the number of T_m intervals in one day.

The number of C_n coefficients in 25 should be within the Nyquist limits to eliminate the potential for aliasing. While C_n are complex numbers and introduce $2n$ variables, half of these may be eliminated so as to match the total number of available SCUC outputs. The Fourier coefficients are pairwise complex conjugates and C_0 is pure real. Also, for the n corresponding to Nyquist frequency, the real part of $f_n(t)$ is a half period cosine in T_h interval and its integration always returns zero. To avoid singularities, the corresponding coefficient is excluded.

In order to solve for the C_n coefficients and tie the ESS schedule to the SCUC Constraint 1 described above must be observed. According to (16), the amount of exchanged energy during interval k is:

$$E_k = S_k T_h \tag{29}$$

To maintain the peak-shaving process and the economical benefits of the SCUC output, the amount of exchanged energy during each time interval should stay the same as in (29):

$$\int_{kT_h}^{(k+1)T_h} S(t)\mathrm{d}t = S_k T_h \tag{30}$$

Thus, integration of the left-hand-side of (25) becomes:

$$\bar{Z}_k = \frac{1}{T_h}\int_{kT_h}^{(k+1)T_h} \left(S(t) + P(t)\right)\mathrm{d}t = S_k + \frac{1}{T_h}\int_{kT_h}^{(k+1)T_h} P(t)\mathrm{d}t \tag{31}$$

and depends on the SCUC output for ESS and the generation schedule, which are known at this point. Integration of the right-hand-side of (25) yields the following:

$$\bar{Z}_k = \frac{1}{T_h}\int_{kT_h}^{(k+1)T_h} \left(\sum_{n=0}^{N-1} C_n \hat{f}_n(t)\right)\mathrm{d}t = \sum_{n=0}^{N-1} C_n \frac{1}{T_h}\int_{kT_h}^{(k+1)T_h} \hat{f}_n(t)\mathrm{d}t \tag{32}$$

Now consider the last term of (32) and define an $n \times n$ matrix $\hat{f}_{nk}$ as

$$\hat{f}_{nk} = \frac{1}{T_h}\int_{kT_h}^{(k+1)T_h} \hat{f}_n(t)\mathrm{d}t \tag{33}$$

Note that $\hat{f}_{nk}$ does not depend on the demand profile and the storage schedule and can be calculated in advance. Equation (32) then takes the following form:

$$Z_k = \sum_{n=0}^{N-1} C_n \hat{f}_{nk} \tag{34}$$

which may be represented as a system of linear equations with C_n unknowns. In matrix form:

$$Z = \hat{F} C \tag{35}$$

From the discussion above, $\hat{F}$ is a square matrix of full rank. Thus, C can be found from the inversion of $\hat{F}$ inversion:

$$C = \hat{F}^{-1} Z \tag{36}$$

After the C_n coefficients are found, the ESS schedule is constructed from (25) and (24):

$$S(t) = \sum_{n=-\infty}^{\infty} c_n \hat{f}_n(t) - P(t) \tag{37}$$

And the state-of-charge becomes:

$$X(t) = X_0 - \int_0^t S(\tau)\mathrm{d}\tau \tag{38}$$

2) Schedule Scaling: The method provided above has yet to explicitly observe the ESS power and energy limits (Constraints 2 & 3). Although the violation may only be marginal, proper scaling of both the power and energy profiles should be performed to ensure the designed schedule can be explicitly followed.

Both power and energy scaling are done with reference to S_k to maintain the relation in (30). For each T_h interval, a scaling parameter α is defined as a ratio of the distance from S_k to the ESS minimum/maximum limits and the maximum deviation of the designed profile from S_k. Each time interval yields scaling parameters for both energy (α_k^E) and power (α_k^P) schedules. However, since the energy and power are related by a linear integration/differentiation operators, scaling one of the profiles also scales the other one. Thus, scaling can be done only once by using the smaller parameter of the two:

$$\alpha_k = \min\left(\alpha_k^E, \alpha_k^P\right) \tag{39}$$

If $\alpha_k \ge 1$, the schedule is within physical limits and is left unchanged. Otherwise, a scaling is implemented as follows:

$$S_k(t) = S_k + \alpha_k\left(S_k(t) - S_k\right) \tag{40}$$

The corresponding SOC profile is found from (38).

a) Power limits: The ESS power schedule should be scaled within S^{min}, S^{max} limits. To this end, the scaling param-

eter for interval k is defined as:

$$\alpha_k^P = \min\left(\frac{S^{max} - S_k}{S_k^{max} - S_k}, \frac{S_k - S^{min}}{S_k - S_k^{min}}\right) \quad (41)$$

where S_k^{max}, S_k^{min} are the maximum and minimum values of $S(t)$ during interval k.

b) Energy limits: According to (38), a constant level S_k in the power domain corresponds to the linear ramp in the energy domain from $X(kT_h)$ to $X((k+1)T_h)$. Using $\bar{X}_k(t)$ notation for the corresponding linear ramp in time interval k, the scaling parameter is defined as:

$$\alpha_k^E(t) = \begin{cases} \frac{X^{max} - \bar{X}_k(t)}{X_k(t) - \bar{X}_k(t)} & \text{if } X_k(t) - \bar{X}_k(t) > 0 \\ \frac{X^{min} - \bar{X}_k(t)}{X_k(t) - \bar{X}_k(t)} & \text{if } X_k(t) - \bar{X}_k(t) < 0 \end{cases} \quad (42)$$

$$\alpha_k^E = \min\left(\alpha_k^E(t)\right) \quad (43)$$

In such a way, an ESS schedule that observes all three previously constraints has been constructed.

IV. Results

The IEEE RTS-96 reliability test system is used as the physical grid [25]. It is composed of three nearly identical control areas, with a total of 73 buses, 99 generators and 8550MW of annual peak load. Wind and load data from the Bonneville Power Administration (BPA) repositories [26] are used for this case study.

The power system operations are simulated for two different scenarios: with and without ESS integrated into the SCUC problem. Fig. 2 shows the SCUC generation scheduling results. As expected, the ESS integration reduces the peak load which also reduces the total generation cost, since the storage allows the accumulation of energy during the off-peak hours and generation during peak hours.

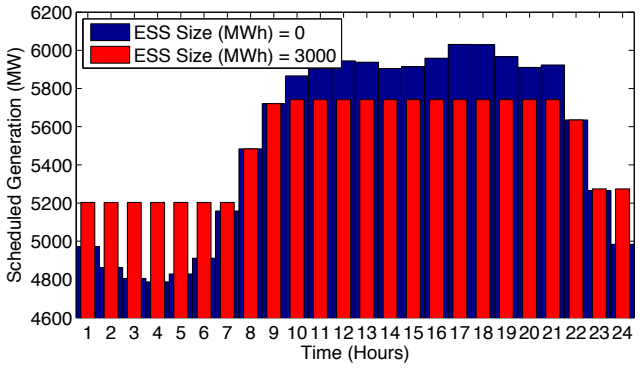

Figure 2: The generation schedule for different storage sizes

The ESS SOC profile scheduled by the SCUC problem is represented in Fig. 3. The graph shows that the ESS starts accumulating energy at the beginning of the day, when the price is also low and returns the energy to the system during peak hours. This pattern matches with the power profiles in Fig. 2. At the end of the operating day, the storage restores its SOC to its initial value. The smooth line in Fig. 3 corresponds to the SOC of the ESS after the smoothing of the power profile

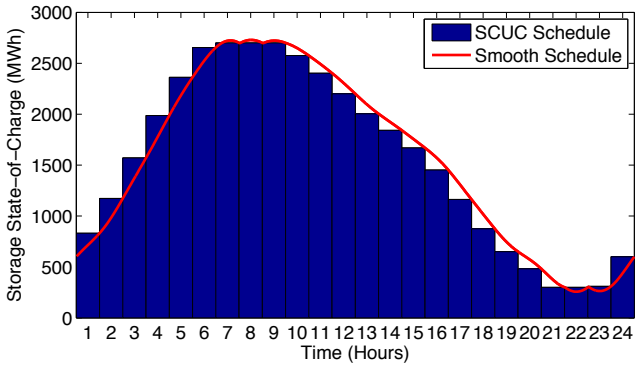

Figure 3: The state-of-charge of the storage

described in Section III is implemented. It should be noted that at the end of each hour the value of the smooth profile is equal to the SOC scheduled by SCUC for the given interval. This is because the initial condition during the smoothing was that the total energy flow from/to ESS during each hour stays equal to the one scheduled by SCUC, reflected in (30).

In order to better understand the impact of ESS on load following reserve requirements, the generation and ESS schedules are compared to the actual demand for the systems with and without ESS integration. Fig. 4 shows that the generation schedule of the system without ESS has a stair-like form, while the total $generation + ESS$ schedule of the system with ESS integration has much smoother form and resembles the actual demand profile much better. This difference defines the

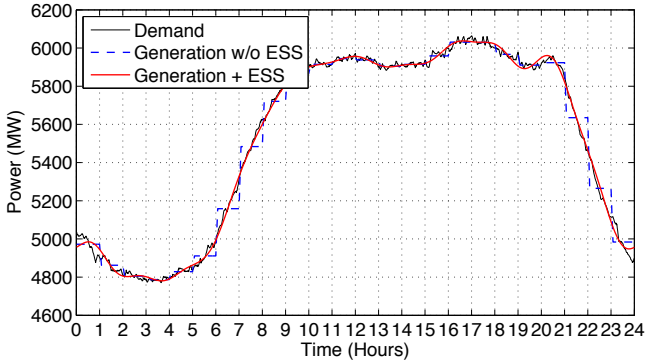

Figure 4: The scheduled generation and storage for two scenarios

actual load following requirements for each system. The load following reserve requirements for both cases are assessed as shown in Fig 5. At the point where the graphs go to saturation corresponds to the reserve requirements of the system and further increase of the reserves does not improve the power balance. The results show that the reserve requirements of the system with ESS integration is significantly lower compared to the traditional system without ESS.

This case study shows that the different timescales of the power system are interconnected. Integration of ESS into the SCUC problem not only helps to shave the peak-load and reduce total operation costs, but also reduces the load following reserve requirements of the system. This phenomenon would be impossible to observe if the study were limited to one time

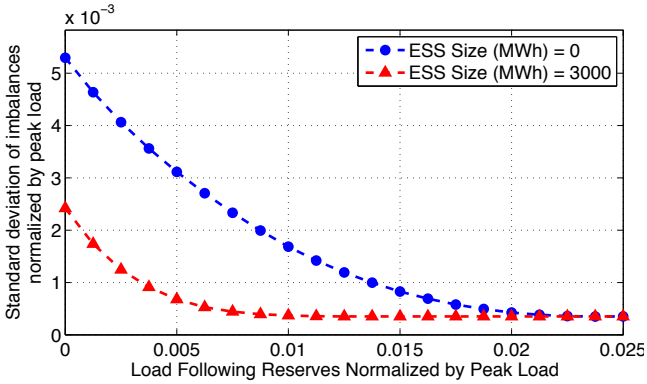

Figure 5: The load following reserve requirements for different storage sizes

scale only. Thus, holistic assessment to assess power system process have been shown to address the interaction of different timescales.

V. Conclusion

In conclusion, this paper has applied the concept of enterprise control to the integration of energy storage systems. While much of the existing ESS literature focuses on a single power grid balancing function, an enterprise control approach includes multiple layers of balancing operations within a single holistic model. As a result, the paper has demonstrated the multiple timescale effects as a consequence of ESS integration into the SCUC. The paper has also developed a novel scheduling technique which beneficially exploits this coupling in two timescales. It simultaneously shows peak-loading shaving and operating costs reductions in the SCUC and load following reserve requirements in the SCED.

References

[1] A. Gomez-Exposito, A. J. Conejo, and C. Cañizares, *Electric Energy Systems: Analysis and Operation*. Boca Raton, Fla: CRC, 2008.

[2] A. M. Farid and A. Muzhikyan, "The Need for Holistic Assessment Methods for the Future Electricity Grid," in *GCC Power 2013 Conference & Exhibition*, Abu Dhabi, UAE, 2013, pp. 1–13.

[3] A. Muzhikyan, A. M. Farid, and K. Youcef-Toumi, "Variable energy resource induced power system imbalances: A generalized assessment approach," in *Technologies for Sustainability (SusTech), 2013 1st IEEE Conference on*, Portland, OR, 2013, pp. 250–257.

[4] ——, "Variable energy resource induced power system imbalances: Mitigation by increased system flexibility, spinning reserves and regulation," in *Technologies for Sustainability (SusTech), 2013 1st IEEE Conference on*, Portland, OR, 2013, pp. 15–22.

[5] F. Diaz-Gonzalez, A. Sumper, O. Gomis-Bellmunt, and R. Villafafila-Robles, "A review of energy storage technologies for wind power applications," *Renewable and Sustainable Energy Reviews*, vol. 16, no. 4, pp. 2154–2171, 2012. [Online]. Available: http://www.sciencedirect.com/science/article/pii/S1364032112000305

[6] M. Beaudin, H. Zareipour, A. Schellenberglabe, and W. Rosehart, "Energy storage for mitigating the variability of renewable electricity sources: An updated review," *Energy for Sustainable Development*, vol. 14, no. 4, pp. 302–314, Dec. 2010. [Online]. Available: http://www.sciencedirect.com/science/article/pii/S0973082610000566

[7] H. Daneshi and A. K. Srivastava, "Security-constrained unit commitment with wind generation and compressed air energy storage," *Generation, Transmission & Distribution, IET*, vol. 6, no. 2, pp. 167–175, 2012.

[8] M. Nazari, M. Ardehali, and S. Jafari, "Pumped-storage unit commitment with considerations for energy demand, economics, and environmental constraints," *Energy*, vol. 35, no. 10, pp. 4092–4101, Oct. 2010. [Online]. Available: http://dx.doi.org/10.1016/j.energy.2010.06.022

[9] Y. Hida, R. Yokoyama, J. Shimizukawa, K. Iba, K. Tanaka, and T. Seki, "Load following operation of NAS battery by setting statistic margins to avoid risks," in *Power and Energy Society General Meeting, 2010 IEEE*, 2010, pp. 1–5.

[10] M. Chhabra, T. Harnesswalla, M. Lim, and F. Barnes, "Frequency regulation and economic dispatch using integrated storage in a hybrid renewable grid," in *Energy, Automation, and Signal (ICEAS), 2011 International Conference on*, ser. Proceedings of the 2011 International Conference on Energy, Automation, and Signal (ICEAS 2011), Bhubaneswar, Odisha, 2011, pp. 1–6. [Online]. Available: http://dx.doi.org/10.1109/ICEAS.2011.6147119

[11] A. Muzhikyan, A. M. Farid, and K. Youcef-Toumi, "An Enhanced Method for the Determination of Load Following Reserves," in *American Control Conference 2014 (ACC2014)*, Portland, OR, 2014, pp. 1–8.

[12] ——, "An Enhanced Method for Determination of the Ramping Reserves," in *Submitted to: 53th IEEE Conference on Decision and Control*, Los Angeles, CA, 2014, pp. 1–8.

[13] S. Dutta and R. Sharma, "Optimal storage sizing for integrating wind and load forecast uncertainties," in *Innovative Smart Grid Technologies (ISGT), 2012 IEEE PES*, 2012, pp. 1–7.

[14] Y. Yang, H. Li, A. Aichhorn, J. Zheng, and M. Greenleaf, "Sizing Strategy of Distributed Battery Storage System With High Penetration of Photovoltaic for Voltage Regulation and Peak Load Shaving," *Smart Grid, IEEE Transactions on*, vol. 5, no. 2, pp. 982–991, 2014.

[15] P. Kundur, N. J. Balu, and M. G. Lauby, *Power system stability and control: The EPRI power system engineering series*. New York: McGraw-Hill, 1994.

[16] S. Frank and S. Rebennack, "A Primer on Optimal Power Flow: Theory, Formulation, and Practical Examples," Colorado School of Mines, Tech. Rep. October, 2012.

[17] J. Carpentier, "Contribution to the economic dispatch problem," *Bull. Soc. Franc. Electr.*, vol. 3, no. 8, pp. 431–447, 1962.

[18] B. Stott, J. Jardim, and O. Alsaç, "DC Power Flow Revisited," *Power Systems, IEEE Transactions on*, vol. 24, no. 3, pp. 1290–1300, 2009.

[19] A. J. Wood and B. F. Wollenberg, *Power generation, operation, and control*, 2nd ed. New York: J. Wiley & Sons, 1996.

[20] K.-S. Kim, L.-H. Jung, S.-C. Lee, and U.-C. Moon, "Security Constrained Economic Dispatch Using Interior Point Method," in *Power System Technology, 2006. PowerCon 2006. International Conference on*, 2006, pp. 1–6.

[21] L. S. Vargas, V. H. Quintana, and A. Vannelli, "A Tutorial Description of an Interior Point Method and Its Applications to Security-Constrained Economic Dispatch," *Power Systems, IEEE Transactions on*, vol. 8, no. 3, pp. 1315–1324, 1993.

[22] H. Saadat, *Power System Analysis*. McGraw-Hill, 1999.

[23] A. Muzhikyan, A. M. Farid, and K. Youcef-Toumi, "An Enterprise Control Assessment Method for Variable Energy Resource Induced Power System Imbalances. Part 1: Methodology," *Submitted to: IEEE Transactions on Industrial Electronics*, vol. 1, no. 1, pp. 1–8, 2014.

[24] ——, "An Enterprise Control Assessment Method for Variable Energy Resource Induced Power System Imbalances. Part 2: Results," *Submitted to: IEEE Transactions on Industrial Electronics*, vol. 1, no. 1, pp. 1–8, 2014.

[25] C. Grigg, P. Wong, P. Albrecht, R. Allan, M. Bhavaraju, R. Billinton, Q. Chen, C. Fong, S. Haddad, S. Kuruganty, W. Li, R. Mukerji, D. Patton, N. Rau, D. Reppen, A. Schneider, M. Shahidehpour, and C. Singh, "The IEEE Reliability Test System-1996. A report prepared by the Reliability Test System Task Force of the Application of Probability Methods Subcommittee," *Power Systems, IEEE Transactions on*, vol. 14, no. 3, pp. 1010–1020, 1999.

[26] Bonneville Power Administration, "Wind Generation & Total Load in The BPA Balancing Authority." [Online]. Available: http://transmission.bpa.gov/business/operations/wind/